Density-functional study of small and medium-sized As_n clusters up to $n=28$

Jijun Zhao*
State Key Laboratory of Materials Modification by Laser, Electron, and Ion Beams & College of Advanced Science and Technology, Dalian University of Technology, Dalian 116024, China
and Institute for Shock Physics, Washington State University, Pullman, Washington 99164, USA

Xiaolan Zhou and Xiaoshuang Chen
National Laboratory for Infrared Physics, Shanghai Institute of Technical Physics, Chinese Academy of Sciences, Shanghai 224502, China

Jinlan Wang
Department of Physics, Southeast University, Nanjing 210096, China

Julius Jellinek
Chemistry Division, Argonne National Laboratory, Argonne, Illinois 60439, USA
(Received 8 July 2005; revised manuscript received 10 January 2006; published 20 March 2006)

Results of an all-electron density functional theory study of structural and electronic properties of As_n clusters in the size range $n \leqslant 28$ are presented and discussed. The atomization energies for most even-sized As_n ($n \geqslant 8$) clusters with closed-shell electronic configurations are higher than that of As_4, indicating their relative stability upon dissociation into As_4 fragments. Similar to P_n clusters, supercluster structures based on As_4, As_6, As_8 units and As_2 bridge were found to be dominant for the larger As_n with $n \geqslant 14$. The size-dependent physical properties of clusters such as atomization energies, ionization potentials, and molecular orbital gaps have been discussed.

DOI: 10.1103/PhysRevB.73.115418 PACS number(s): 36.40.Cg, 36.40.Mr

I. INTRODUCTION

As a component of GaAs, arsenic plays an important role in semiconductor industry. During the molecular beam epitaxy (MBE) growth of GaAs-based materials, incorporation of arsenic atoms and adsorption of small As clusters on GaAs surface are important to the growth mechanism.[1–4] Therefore, studies of structural and electronic properties of As clusters are interesting in fundamental cluster physics[5–7] and of potential practical relevance to the semiconductor industry.

The configuration of the valence electrons of As, as a group 15 element, is of the s^2p^3 type. To form a complete eight-electron closed-shell, atoms of group 15 elements tend to form three single bonds with the neighboring atoms. In their vapor phase, they form tetrahedral tetramers with three single bonds per atom. In their bulk structures,[8] atoms of group 15 elements are usually bonded to three neighbors, forming covalent networks.

Experimental studies focused on As_n clusters of small sizes (up to n=5).[9–19] Dissociation energies of anionic As_n were determined from appearance potentials and translational energies of the As^-, As^{2-}, and As^{3-} ions formed by electron-impact induced dissociation of As_4.[9] Raman spectroscopy was employed to study the vibrational modes of As_4.[11,12] The electronic structure of the cationic and anionic clusters was investigated using photoelectron spectroscopy,[13–17] whereas the ionization potentials of the neutral As_n were determined through photoionization mass spectrometry[18] and gas-phase charge-transfer reactions.[19]

Most theoretical studies also considered small As_n clusters ($n \leqslant 6$).[20–27] In a Hartree Fock Moller-Plesset 2nd (HF)/(MP2) treatment, a cagelike structure with D_{3d} symmetry was considered for As_{12} and a dodecahedral conformation with I_h symmetry was explored for As_{20}.[27] Low-energy configurations were obtained for As_n, $n \leqslant 11$, using simulated annealing and the local density approximation (LDA) within the density-functional theory (DFT).[26] A gradient-corrected version of DFT was employed to explore some fullerene cage structures for As_n, $n=20$, 28, 32, 36, and 60, and to analyze their stability with respect to As_4.[28] In addition to homogeneous As_n, onionlike $[As@Ni_{12}@As_{20}]^{3-}$ clusters were investigated experimentally[29] and in DFT computations.[30,31]

The goal of this study is to explore structural and electronic properties of As_n clusters in the size range $6 \leqslant n \leqslant 28$. Our broader aim is to identify general trends in the size evolution of clusters of group 15 elements. In particular, we analyze the properties of As_n clusters in comparison with those of P_n clusters.[32,33] As in Refs. 32 and 33, we mainly concentrate on even-numbered clusters for $n \geqslant 6$. The next section outlines the computational methodology. The results and discussion are presented in Sec. III. A brief summary is given in Sec. IV.

II. COMPUTATIONAL METHODOLOGY

The optimization of the cluster structures was performed using DFT with the Perdew-Burke-Ernzerhof (PBE) exchange-correlation functional[34] and an all-electron basis set of the double-numerical-plus-*d*-polarization (DND) type, as implemented in the DMOL package.[35] Only the lowest

TABLE I. Bond lengths, atomization energies, and vibration frequencies of As_2 dimer and As_4 tetramer from experiments (Refs. 40, 9, and 12) and current all-electron DFT computations using PBE functional and DND basis set.

	As_2 dimer			As_4 dimer				
	d_0 (Å)	AE (eV)	ω_0 (cm^{-1})	d_0 (Å)	AE (eV)	ω_1 (cm^{-1})	ω_2 (cm^{-1})	ω_3 (cm^{-1})
Expt.	2.103	3.948±0.023	430	2.435	10.281±0.095	200.8	251.0	342.0
PBE	2.142	4.074	423.5	2.495	10.74	197.8	251.6	341.7

spin-multiplicity state (i.e., singlet for even-numbered clusters, doublet for odd-numbered clusters) was considered. The energy and electron density were converged to within 10^{-6} a.u., the forces to within 2×10^{-3} a.u. The structures were optimized with no symmetry constraints imposed. Normal mode analysis was performed for the most stable structure of each cluster size and some low-energy metastable isomers (6*b* in Fig. 2, 10*b* in Fig. 4, 16*b* and 16*c* in Fig. 7). Except 16*b* and 16*c*, each of which has one small imaginary frequency, no imaginary frequencies were found for these lowest-energy and metastable configurations, indicating they are true minima of potential energy surface.

The DFT optimizations for As_n, $n\leqslant18$, were carried out using a number of different initial configurations (typically more than 20) generated in two ways. In the first, we used the Stillinger-Weber (SW) potential[36] with parameters for As-As interaction given in Ref. 47, and employed a genetic algorithm (GA)[37–40] to obtain low-energy configurations. Some pioneering works have demonstrated its impressive efficiency in searching the global minima of clusters as compared to standard simulated annealing.[37] In the GA procedure, we generated N_p of initial configurations by random (typically, $N_p=16$, depending on cluster size). Any two candidates in this population can be chosen as parents to produce a child cluster through a crossover process and optionally a mutation operation. The child cluster from each generation was relaxed with SW empirical potential, and then it was selected to replace its parent in the population if it has lower energy. Typically, 1000 GA iterations are suffcient to ensure a truly global search up to $n=18$.

In the second, we employed the structural forms obtained in earlier studies for P_n clusters.[41,32,33] Analogy with the latter also was the guiding principle in construction of the "supercluster" structures for larger As_n, $n=20$, 24, and 28. In this size range ($n=20-28$), we only considered a few structural candidates of supercluster structure and fullerene cages for each size.

The degree of adequacy of the computational framework (PBE/DND) specified above can be assessed from comparison of the results of earlier theoretical studies and the available experimental data for smaller As_n clusters with $n=2-6$, as we will show in the next section.

III. RESULTS AND DISCUSSIONS

Using the computation scheme described in Sec. II, we have explored a number of low-lying isomers and determined the lowest-energy structure for As_n clusters up to $n=18$, which were shown in Figs. 1–8. For the larger As_n clusters, such as As_{20}, As_{24}, and As_{28}, we focused on the supercluster structures and some of them are shown in Fig. 9. Our results on small As_2 and As_4 clusters were compared with experiments in Table I as benchmark. The physical properties of the As_n clusters such as atomization energy, highest energy occupied molecular orbital (HOMO)-lowest energy unoccupied molecular orbital (LUMO) gap, and ionization potential were calculated and the results were presented in Table II and Figs. 10 and 11. The details of our theoretical results will be presented in the following.

A. As_{2-5}

The bond lengths, atomization energies, and vibration frequencies of As_2 dimer and As_4 tetramer have been measured in previous experiments[9,12,42] and can be critical benchmarks for testing the accuracy of current theoretical methods. As shown in Table I, the overall agreement between theory and experiments for both As_2 and As_4 are quite good. For As_2 dimer, our theoretical bond length (2.142 Å), atomization energy (4.074 eV), and vibration frequency (423.5 cm^{-1}) compare well with the experimental data (2.103 Å, 3.948 eV, 430 cm^{-1}).[9,42] The current PBE/DND calculations overestimate the As-As bond length in As_2 by about 0.04 Å. Similar overestimation of bond length was found for As_4 (see Table I).

An isosceles triangle (C_{2v}) with apex angle $\alpha=65.18°$ and side length $r=2.359$ Å was found as ground state structure for As_3. The present geometry parameters for As_3 are close to previous DFT calculations,[20,22,23] such as $r=2.332$ Å and $\alpha=65.00°$ in Ref. 22. The energy of isosceles triangle (C_{2v}) is lower than the equilateral triangle (D_{3h}) by 0.09 eV, whereas previous LDA calculations by Ballone and Jones predicted a $\Delta E=0.09$ eV between C_{2v} and D_{3h} triangle structures.[26] Moreover, our theoretical atomization energy (2.140 eV per atom) of As_3 is consistent with the experimental data (2.135±0.247 eV per atom)[9] quite well.

In the case of As_4, the energy of ground-state tetrahedron (T_d) structure is lower than that of a square (D_{4h}) by 2.13 eV and a planar rhombus (D_{2h}) by 2.53 eV. Such significant energy difference between the three-coordinated tetrahedron and the planar structures with a lower coordination number $CN=2$ or 2.5 indicates strong tendency of forming three single covalent bonds for each As atom. Since As_4 is the most prominent species in arsenic vapor, there have been a number of experimental and theoretical studies on As_4 cluster. As shown in Table I, our theoretical vibration frequencies agree very well with experiments,[9,10] with average deviation of 1.3 cm^{-1}. The energy for As_4 dissociating into two As_2 is

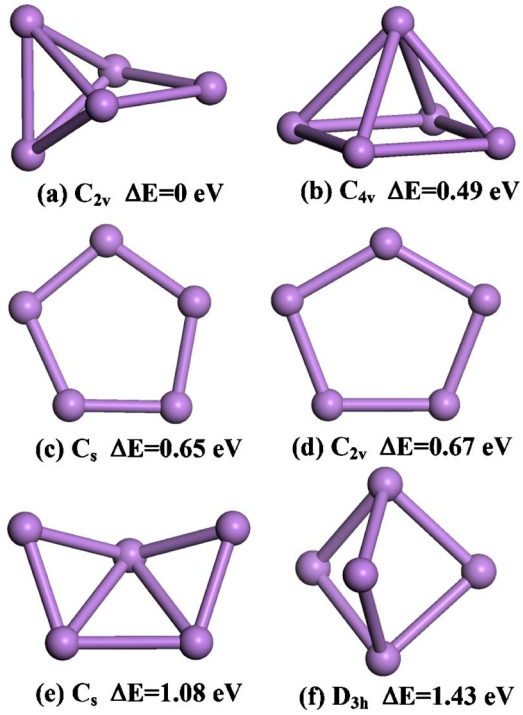

FIG. 1. (Color online) Low energy isomers of As_5 cluster.

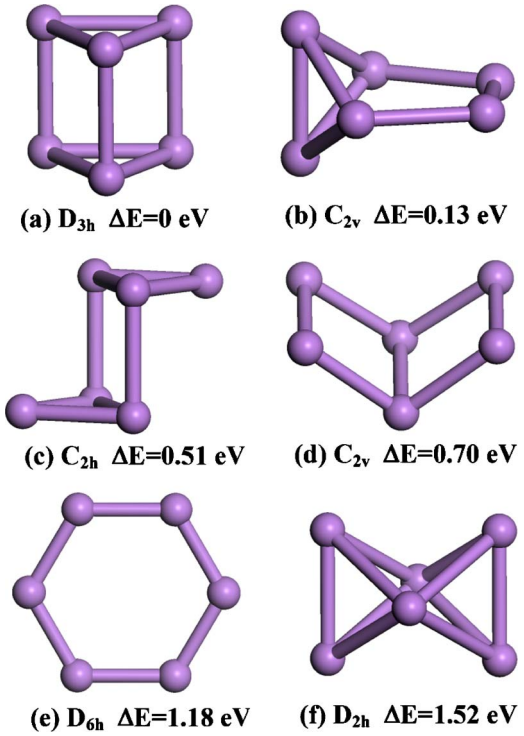

FIG. 2. (Color online)Low energy isomers of As_6 cluster.

2.592 eV from our PBE calculation, while experimental data is 2.353 ± 0.048.[9] In previous theoretical works, the computed As-As bond length of As_4 tetrahedron ranges from 2.42 Å to 2.50 Å.[21,23,26–28] Our PBE bond length 2.495 Å falls in this range and is on the upper bound. Again, comparison with experimental bond length 2.435 Å (Ref. 10) shows that the current PBE calculations somewhat overestimate the As-As bond length in arsenic clusters.

As shown in Fig. 1(a), the lowest energy structure of As_5 has a C_{2v} symmetry and can be viewed as an edge-caped distorted tetrahedron with one broken side. This result agrees with previous theoretical calculations.[26,23] The square pyramid with C_{4v} symmetry in Fig. 1(b) was found to be a low-lying isomer, with 0.49 eV higher than the ground state, in agreement with previously predicted $\Delta E = 0.43 - 0.79$ eV using different density functional.[23] The planar pentagonal five-membered ring (5MR) with D_{5h} symmetry has exactly degenerated HOMO and LUMO. John-Teller effect leads to distortion away from D_{5h} to lower symmetric structures, either a near-planar C_s isomer [Fig. 1(c)] or a planar C_{2v} isomer [Fig. 1(d)]. The energy difference between planar C_{2v} isomer [Fig. 1(d)] and the global minimum is 0.67 eV from present PBE calculation, while previous DFT calculations gave $\Delta E = 0.31 - 0.87$ eV.[23] Starting from planar trapezia structure with C_{2v} symmetry, the cluster transformed into a three-dimensional isomer with C_s symmetry [Fig. 1(e)] upon relaxation. The trigonal bipyramid structure with D_{3h} symmetry in Fig. 1(f) has been considered but its energy is much higher than that of the ground state by $\Delta E = 1.43$ eV.

B. As_6

Two low-lying structures that are very close in energy were found for As_6, one with D_{3h} symmetry [Fig. 2(a)], another with C_2 symmetry [Fig. 2(b)]. The trigonal prism (D_{3h}) in Fig. 2(a) was found as ground-state structure and is only 0.13 eV lower than the C_{2v} isomer in Fig. 2(b). Similar to the ground-state structure of As_5 [Fig. 1(a)], the C_{2v} structure of As_6 in Fig. 2(b) can be viewed as a distorted tetrahedron edge-capped by a As_2 dimer on the open edge. In a previous work, the analogy of As_6 cluster and valence isomers of benzene was investigated by Warren *et al.* using restricted Hartree-Fock method with 6-311G** basis.[25] They also found that the energy of D_{3h} structure [Fig. 2(a)] is lower than that of C_{2v} isomer [Fig. 2(b)] by $\Delta E = 0.24$ eV, which is close to our result ($\Delta E = 0.13$ eV). On the contrary, Ballone and Jones predicted the C_{2v} isomer is slightly more stable than D_{3h} isomer by only 0.06 eV.[26]

As for the other structural isomers of As_6, the C_{2h} structure in Fig. 2(c) has never been considered for As_6, and its energy is 0.51 eV higher than the D_{3h} ground state. The C_{2v} structure in Fig. 2(d) was investigated in Ref. 25 with $\Delta E = 0.92$ eV, while ΔE is 0.70 eV from present PBE calculation. The planar hexgonal six-membered ring (6MR) with D_{6h} symmetry in Fig. 2(e) was also considered in previous works.[24,25] The energy difference ΔE between the hexagonal ring (D_{6h}) and the ground-state trigonal prism (D_{3h}) is 1.18 eV from present calculation, while $\Delta E = 0.99$ eV in Ref. 24 and $\Delta E = 1.98$ eV in Ref. 25.

C. As_8

As shown in Fig. 3(a), the cagelike structure with C_{2v} symmetry was obtained as the lowest energy structure for As_8. This result agrees with previous work of LDA simulated annealing by Ballone and Jones.[26] In Ref. 26, the D_{2h} iso-

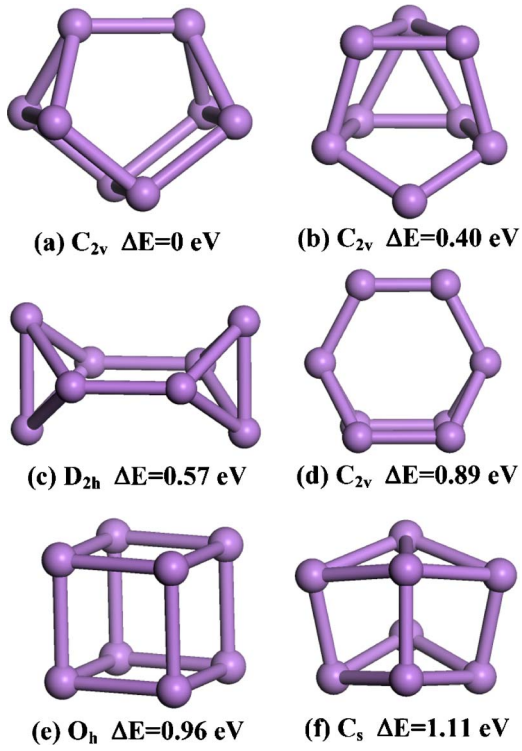

FIG. 3. (Color online) Low energy isomers of As_8 cluster.

mers [Fig. 3(c)] was also obtained as a less stable isomer with $\Delta E=0.32$ eV, while our PBE calculations predict a $\Delta E=0.57$ eV. For the isomer with cubic structure (O_h) in Fig. 3(e), Ballone predicted a $\Delta E=1.36$ eV with regard to the ground state, while is $\Delta E=0.96$ eV within our approach. The As_8 cube in Fig. 3(e) was recently studied by Baruah.[28] Their theoretical bond length 2.547 Å (Ref. 28) is very close to present PBE bond length 2.563 Å. For all of the structural isomers studied, we found that arsenic atoms tend to connect with other three atoms by a single covalent bond [see Figs. 3(a), 3(c), 3(e), and 3(f)]. Moreover, as we will show later, the lowest energy structures of As_4 (tetrahedron, T_d), As_6 (trigonal prism, D_{3h}), and As_8 (cage structure, C_{2v}) serve as primary building units for forming the As clusters of larger sizes.

D. As_{10}

The C_s structure in Fig. 4(a) was found as the lowest energy structure of As_{10} clusters. It can be viewed as the ground-state cage structure of As_8 edge-caped by a As_2 dimer on one broken side bond. The same ground-state structure was found by Ballone and Jones for As_{10}.[26] The C_{2v} structure in Fig. 4(b) is composed of two distorted As_4 tetrahedrons connected by an As_2 bridge and its energy is only 0.07 eV higher than the ground-state structure. Among the other structural isomers, the C_s structure in Fig. 4(d) can be considered as a supercluster of As_4 and As_6 units. The C_{2h} structure in Fig. 4(g) can be viewed as two distorted As_4 tetrahedrons connected by an As_2 bridge, or two directly connected As_5 with edge-capped tetrahedron structure. The C_{2v} structure in Fig. 4(e) is formed by edge-capping As atoms on the two sides of C_{2v} cage of As_8. It is interesting to find the early stage of fullerene cage in the C_{3v} structure [Fig. 4(c)], which contains three four-membered rings (4MR) and three five-membered rings (5MR). As we will see in the following discussions, fullerenelike cage structures consisting of 4MRs and 5MRs were always found as low-lying isomers for the As_n with $n \geqslant 10$.

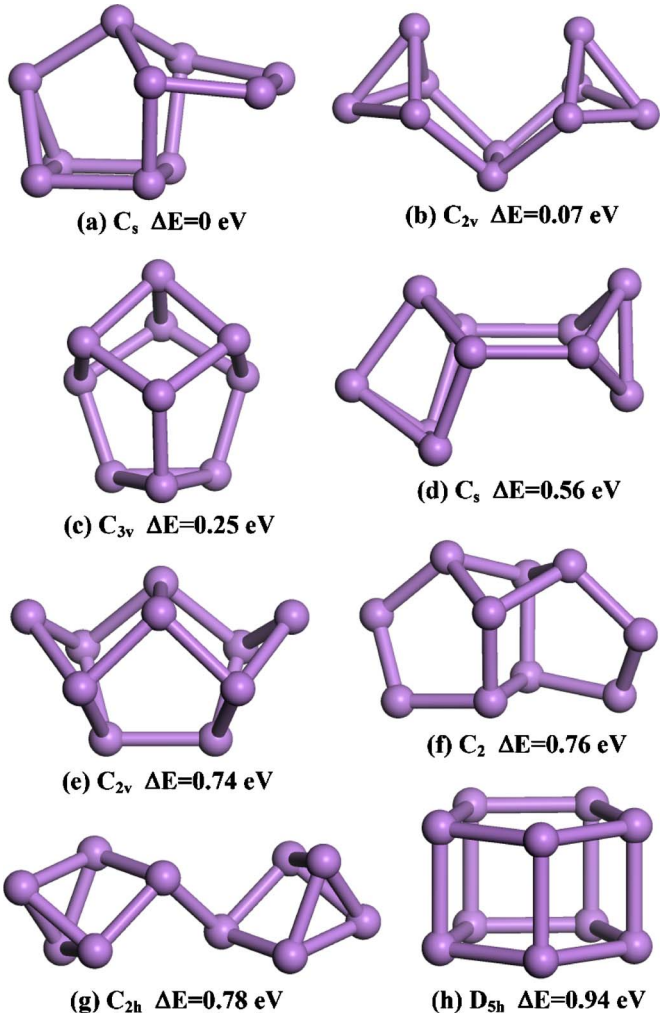

FIG. 4. (Color online) Low energy isomers of As_{10} cluster.

E. As_{12}

In analogy to P_{12}, a cagelike D_{3d} structure of three layers of atoms (3+6+3) was considered for As_{12} in a previous study.[27] This D_{3d} structure [Fig. 5(a)] was confirmed to be the lowest energy structure among all the structural candidates considered in present study. Several low-lying isomers, such as those in Fig. 5(b) (C_s), Fig. 5(c) (C_s), and Fig. 5(g) (D_{2d}) can be viewed as superclusters based on As_8 unit, connected to an As_4 unit in either tetrahedral structure [C_s isomer in Fig. 5(b), and D_{2d} isomer in Fig. 5(g)] or square structure [C_s isomer in Fig. 5(c)], or edge-capped by two As_2 on the two sides [C_{2v} isomer in Fig. 5(e)]. Similar to the C_{3v} structure for As_{10} [Fig. 4(c)], we obtained a cage with D_{2d} symmetry [Fig. 5(d)], which contains four 4MRs and four

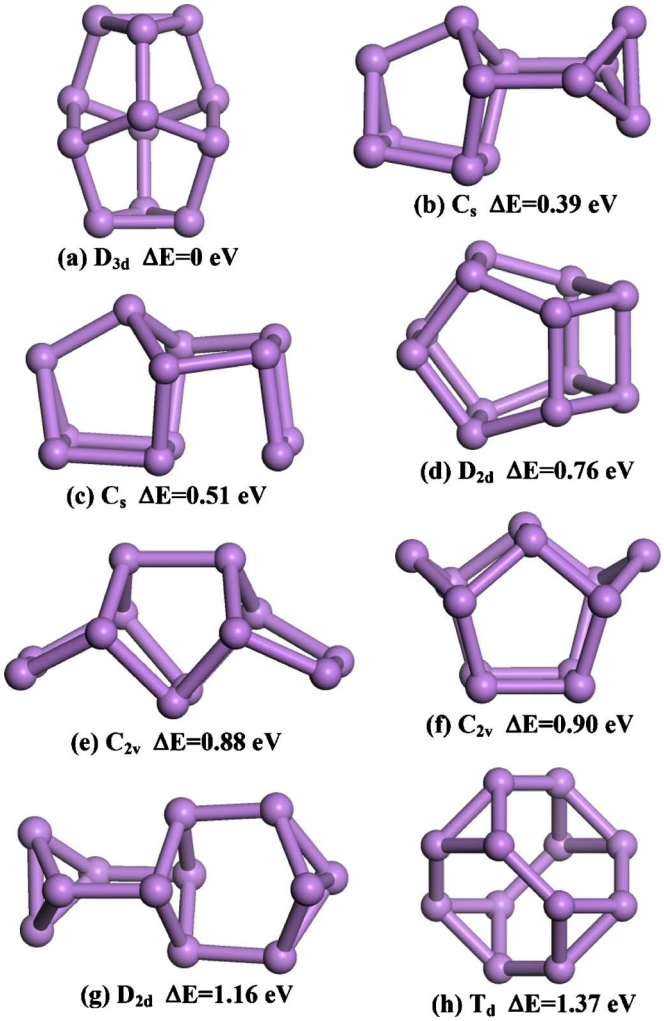

FIG. 5. (Color online) Low energy isomers of As_{12} cluster.

5MRs. On the other hand, a high-symmetry T_d isomer in Fig. 5(h) was found, which is formed by four three-membered rings and four six-member rings (6MR).

F. As_{14}

Starting from As_{14}, supercluster structures built by As_8 and As_4 units were found to be the dominant structural pattern for the lowest energy structures. In addition to As_8 and As_4 units, supercluster structures built by As_6 unit were also found as low-lying isomers for As_n clusters with $n \geqslant 14$. As shown in Fig. 6(a), the ground-state structure of As_{14} (C_s symmetry) consists of an As_8 unit and an As_4 unit, linked by an As_2 bridge. Similarly, the C_{2v} isomer in Fig. 6(b) is built by two identical As_6 units with an As_2 bridge in the middle. Cage structures with 4MR, 5MR, and 6MR were found as low-lying isomers for As_{14} with $\Delta E > 1$ eV, as shown in Figs. 6(c)–6(f). As continuation of the spherical cage structure for As_{12} [Fig. 5(d)], fullerenelike cages were found as the low-lying structures that are shown in Fig. 6(d) and Fig. 6(e). The D_{3h} cage [Fig. 6(d)] contains four 5MR and three 4MR, while the C_{2v} cage [Fig. 6(e)] has one 6MR, two 5MR, and four 4MR. Two other nonspherical cages with lower symmetry like C_2 [Fig. 6(c)] or C_s [Fig. 6(f)], were also found as low-energy isomers for the As_{14} cluster.

G. As_{16}

For As_{16}, several supercluster structures of As_8 and As_6 units were found as low-lying isomers. As shown in Fig. 7, the combination of those superclusters [Figs. 7(a)–7(e)] can be considered as As_8-As_8 [7(a) C_{2h}, 7(b) C_s, 7(e) C_s], As_8-As_2-As_6 [7(c) C_s], and As_6-As_2-As_2-As_6 [7(d) C_{2v}], respectively. Among those supercluster structures, it seems that the As_8 building unit is more energetically favorable. Both the C_{2h} ground state structure in Fig. 7(a) and the nearly degenerate C_s isomer (with $\Delta E = 0.04$ eV) in Fig. 7(b) are composed of two As_8 units, which are connected with each other in two different orientations. On the other hand, the D_{4d} cage in Fig. 7(f) was found as an isomer with $\Delta E = 1.23$ eV, which contains eight 5MR and two 4MR. It can be also viewed as a 4+8+4 three-layered structure, similar to the 3+6+3 three-layered ground-state structure for As_{12} [Fig. 5(a)].

H. As_{18}

In the cases of As_{18}, we found coexistence of several structural patterns. The lowest energy structure in Fig. 8(a) with C_{2v} symmetry is built by two identical As_8 units and an As_2 bridge in the middle. The structural isomers in Fig. 8(c) and Fig. 8(d) are based on the D_{3d} ground-state structure of As_{12} [Fig. 5(a)], one is built as As_{12}-As_2-As_4 [Fig. 8(c)] and another one can be considered as a superstructure of As_{12} and As_6 [Fig. 8(d)]. The D_{3h} isomer in Fig. 8(b) can be viewed as a 3+6+6+3 layered structure that is similar to the 3+6+3 layered structure for As_{12} [Fig. 5(a)]. Spherical cage structure was also found in the C_{2v} isomer in Fig. 8(e), which has one 6MR, eight 5MR, and two 4MR. Indeed, this structure can be considered as an truncated fullerene cage from As_{20}. Although there are several competing structural patterns, the energy of the supercluster structure based on As_8 units in Fig. 8(a) is obviously lower than the other possible structural candidates.

I. Comparison to P_n clusters

In previous optimization of small As_n ($n=2-11$) clusters using simulated annealing technique, it was found that the structures of As_n clusters are characterized by an almost uniform ~9% expansion of the corresponding P_n structures. In this work, the same lowest energy structures were found for As_n and P_n clusters at $n=3$, 4, 5, 8, 12, 14, 16, and 18.[41,32,33] In the cases of $n=6$ and 10, there are several minimum structures on the potential energy surface that are very close in energy ($\Delta E \sim 0.1$ eV). Our PBE calculation found that the trigonal prism with D_{3h} symmetry [Fig. 2(a)] as lowest energy structure for As_6, while the C_{2v} structure in Fig. 2(b) was predicted as the lowest energy structure for P_6 in previous first-principles calculations using different methods.[41,32,33] For $n=10$, the C_{2v} structure in Fig. 4(b) was found to be energetically favorable for P_{10},[41,32,33] while both our PBE calculation and previous DFT study indicated that

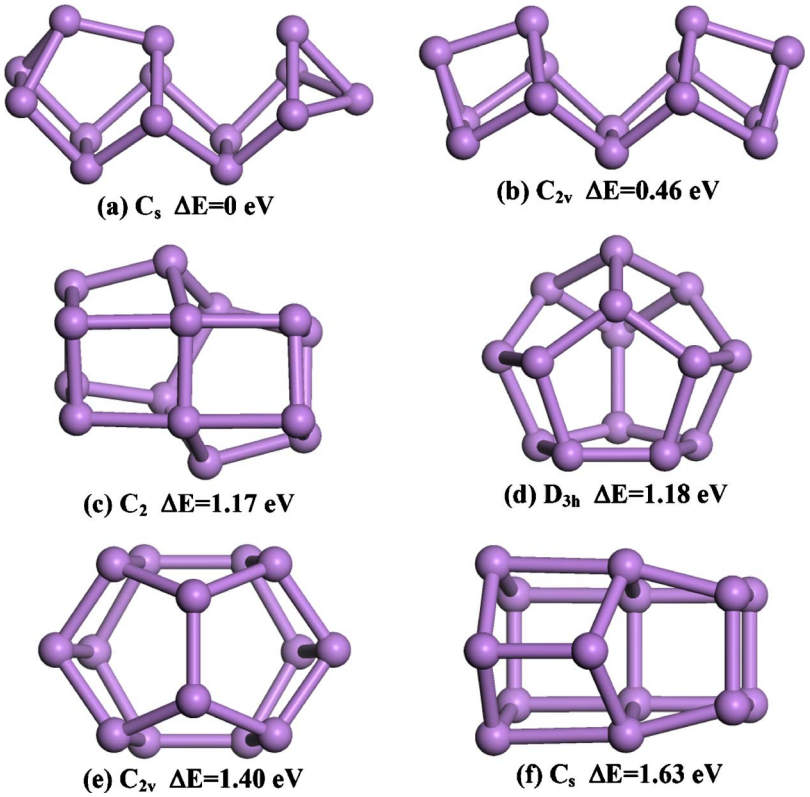

FIG. 6. (Color online) Low energy isomers of As_{14} cluster.

the C_s structure in Fig. 4(a) is the lowest energy structure. Therefore, although As_n and P_n clusters show substantial similarity in their structural properties, there is still a small difference between the As-As and P-P bonding, which leads to the different energy sequence for the structural isomers at $n=6$ and 10.

J. As_n ($n=20,24,28$) clusters: Supercluster vs fullerene

For the larger As_n clusters, the potential energy surface becomes even more complicated and the number of structural isomers increases rapidly. Thus, it is hard to consider all the possible local minima structures. Based on the above discussions of smaller As_n clusters with $n \leqslant 18$, we focused

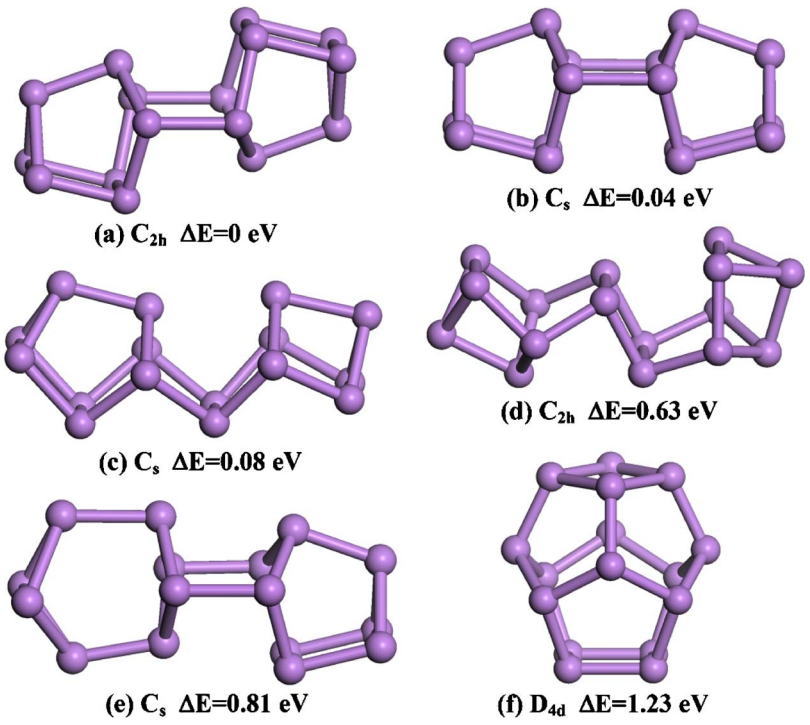

FIG. 7. (Color online) Low energy isomers of As_{16} cluster.

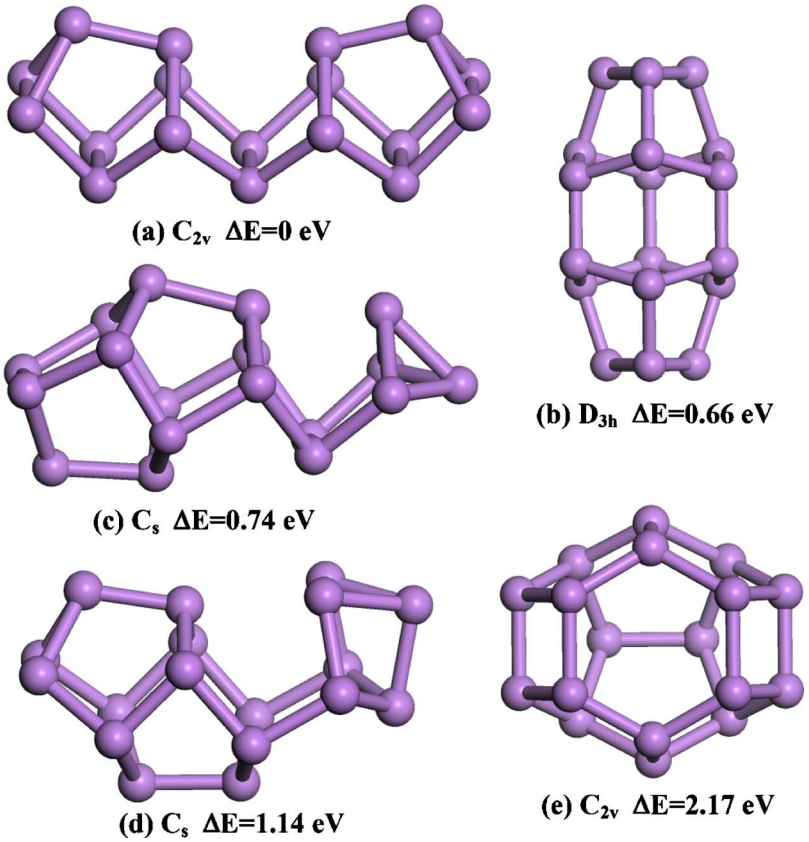

FIG. 8. (Color online) Low energy isomers of As_{18} cluster.

the competition between two kinds of structural patterns for the larger As_n ($n \geqslant 20$), i.e., superclusters vs fullerene cages. Supercluster structures based on As_4, As_6, and As_8 units and As_2 bridges were constructed for As_{20}, As_{24}, and As_{28} clusters. For each size of As_n ($n=20,24,28$) clusters, we considered two to four supercluster structures and the lowest energy one from our calculations is shown in Fig. 9. The optimal combinations of the superclusters are As_4-As_2-As_8-As_2-As_4 for As_{20} [Fig. 9(a)], As_6-As_2-As_8-As_2-As_6 for As_{24} [Fig. 9(b)], and As_8-As_2-As_8-As_2-As_8 for As_{28} [Fig. 9(c)], all with C_{2v} symmetry. Similar supercluster structures have been considered for P_{24} and P_{28} clusters.[32]

The stability of fullerene cages of group 15 elements has been an interesting topic due to their analogy with carbon fullerenes.[43–45,28] In the smaller As_n ($n=10-18$) clusters, cages consisting of 4MR, 5MR, and 6MR were obtained as low-lying structures. Thus, it is natural to further examine the energy and stability of the "classical" fullerene cages formed by 5MR and 6MR of arsenic atoms. For As_{20} and As_{24}, there is only one possible fullerene cage structure for each, with I_h and D_{6d} symmetry respectively. For As_{28}, there are two fullerene cages, one with T_d symmetry and another with D_2 symmetry. Our calculations show that the energy of D_2 cage is about 0.09 eV lower than that of T_d cage. For all the sizes studied, the energies of supercluster structures are substantially lower than that of fullerene cages. The energy difference ΔE between supercluster and fullerene cages become larger as cluster size increases, that is, $\Delta E=0.08$ eV/atom for As_{20}, $\Delta E=0.12$ eV/atom for As_{24}, and $\Delta E=0.18$ eV/atom for As_{28}. The average atomization energies for the As_{20}, As_{24}, and As_{28} cages (2.748, 2.716, 2.691 eV/atom, respectively) are still slightly higher than that of As_4 (2.685 eV/atom). Thus, they might be stabilized by stuffing other guest atoms inside the hollow cage. For example, an onionlike $[As@Ni_{12}@As_{20}]^{-3}$ cluster was

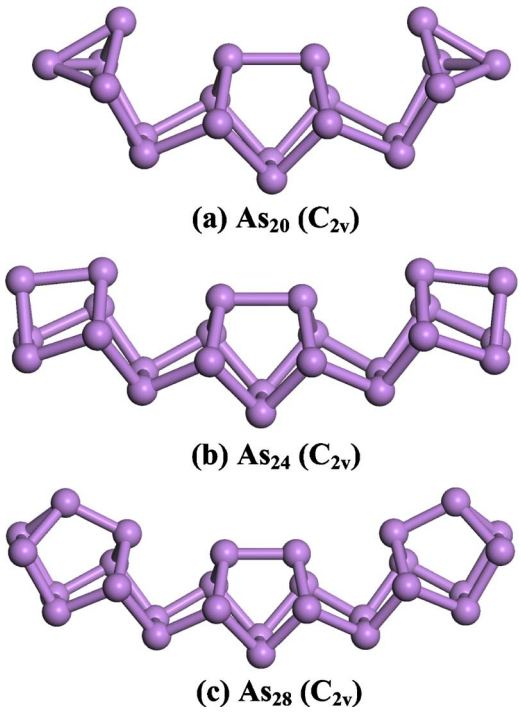

FIG. 9. (Color online) Supercluster structures of As_{20}, As_{24}, and As_{28} clusters.

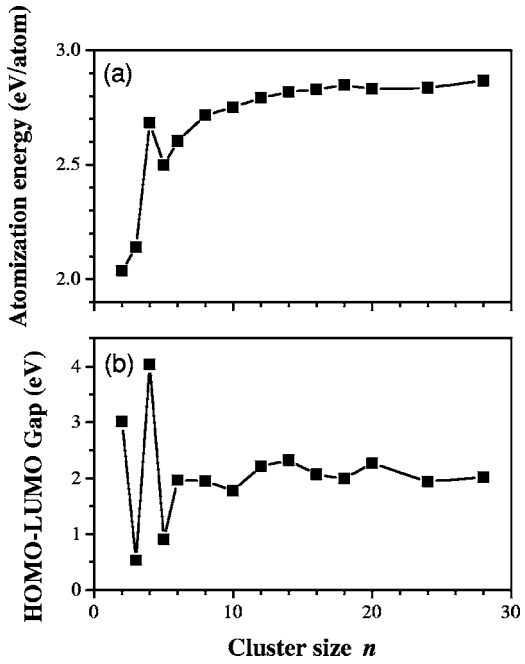

FIG. 10. Atomization energy per atom and HOMO-LUMO gap as function of cluster size of As_n.

found in recent experiment.[29] The finding that fullerenelike shapes of As_n are, by the standard of supercluster structures, increasingly less favored as n grows from 20 to 28 is highly plausible in view of the tendency of As to form three-dimensional as opposed to planar networks. In contrast, medium-sized carbon clusters adopt fullerene structures as embryo of grahite with planar networks by 6MRs.

K. Size dependence of atomization energy and HOMO-LUMO gap

In Fig. 10 we plot the atomization energy per atom and HOMO-LUMO gap for As_n clusters as function of cluster size. First, we find pronounced peaks in both atomization energy and HOMO-LUMO gap at As_4, which is in accord with the high stability and high abundance of As_4 observed experimentally. For the As_n clusters with $n \geqslant 6$, both atomization energy and the HOMO-LUMO gap show smooth size dependent variations. For example, the HOMO-LUMO gap is around 2.0 eV in the size range of $n=6-28$ for all the even-sized clusters, with small deviation of about ±0.3 eV (see Table II). Starting from As_5, the atomization energy also gradually increases from ~2.5 eV to ~2.9 eV (up to As_{28}) as the clusters become larger. As shown in Fig. 10, the stabilized HOMO-LUMO gap after $n=6-8$ is clearly related to the relatively smooth size-dependent change of binding energy in the same size region. This behavior might be associated to the change of chemical bonding in the As clusters. It is also noteworthy that the atomization energy of all the even-sized As_n with $n \geqslant 8$ is higher than that of As_4. Thus, these clusters would remain stable instead of dissociation into small pieces of As_4 if they are synthesized.

In Table II, we compare the theoretical vertical ionization potentials (IPs) and the measured IP from gas-phase charge-transfer reactions.[19] Except for As_5, the theoretical IPs of those small clusters agree with experiments within 4%. There are no experimental results for the larger As_n with $n \geqslant 6$. The size-dependent IPs of As_n clusters are plotted in Fig. 11 as a function of the inverse of cluster radius, $n^{-1/3}$. For smaller clusters, i.e., $n \leqslant 14$, one can see dramatic size-dependent oscillation of the IP. After $n \geqslant 14$, the change of IP with cluster radius becomes rather smooth. A linear fitting of IP to the inverse of cluster radius, $n^{-1/3}$ yields the bulk limit 5.13 eV, compared to the experimental work function 4.72 eV for solid arsenic.[46]

TABLE II. Atomization energies (AE), HOMO-LUMO gap, and ionization potentials (IP) of As_n ($n=2-28$) clusters with lowest-energy structures. The numbers in braket are experimental IP for small As_n ($n=2-5$) clusters, with error bar ±0.10 eV.

n	Symmetry	AE (eV/atom)	Gap (eV)	IP (eV)
2	$D_{\infty h}$	2.037	3.007	9.524 (9.89)
3	C_{2v}	2.140	0.529	7.355 (7.46)
4	T_d	2.685	4.035	8.481 (8.63)
5	C_{2v}	2.499	0.906	7.133 (7.95)
6	D_{3h}	2.603	1.965	7.892
8	C_{2v}	2.717	1.954	7.374
10	C_s	2.752	1.777	7.603
12	D_{3d}	2.793	2.214	7.366
14	C_s	2.819	2.320	6.937
16	C_{2h}	2.830	2.071	6.777
18	C_{2v}	2.849	1.995	6.754
20	C_{2v}	2.832	2.265	6.903
24	C_{2v}	2.837	1.940	6.873
28	C_{2v}	2.867	2.019	6.774

IV. CONCLUSION

In summary, we have performed global search of the lowest-energy structures of As_n ($n=2-6$ and $n=8-18$ of

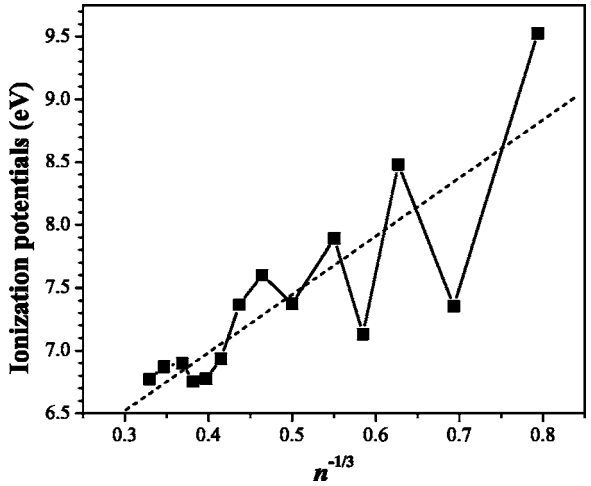

FIG. 11. Ionization potentials as function of the inverse of cluster radius $n^{-1/3}$. The dashed line is a linear fit of IP versus $n^{-1/3}$, which yields a bulk limit of 5.13 eV.

even-sized) clusters by considering a number of structural isomers and employing all-electron DFT calculations for the geometry optimization. The equilibrium structures obtained for smaller As_n ($n=2-12$) cluster are consistent with previous computational results. Starting from As_{14}, we observed competition between structural patterns of fullerenelike cages and superclusters built by As_4, As_6, and As_8 units and an As_2 bridge, while superclusters prevail in energy. These two competing structural growth patterns have been further examined for the larger clusters at As_{20}, As_{24}, and As_{28}. The superclusters become more energetically favorable than fullerene cages as cluster size increases. For most cluster sizes studied, As_n and P_n clusters show almost identical lowest energy structures with exception at $n=6$ and 10. For $n \geqslant 6$, the As_n clusters exhibit smooth size-dependent behavior in atomization energies and HOMO-LUMO gaps. The atomization energies for all the even-sized As_n clusters with $n \geqslant 8$ are higher than that of As_4, indicating the relative stability upon dissociation into As_4 fragments. Although supercluster growth pattern is found to be dominant for the medium-size range with $n=14-28$, it would be interesting to further explore the transition from supercluster structure to bulklike structure of α-As solid in the larger cluster size region.

ACKNOWLEDGMENTS

We acknowledge support from the Office of Naval Research of US (Contract No. N00014-01-1-0802), the Department of Energy of US (Contract No. DEFG0397SF21388), the Office of Basic Energy Sciences, Division of Chemical Sciences, Geosciences, and Biosciences, U.S. Department of Energy (Contract No. W-31-109-Eng-38), and the Chinese National Science Foundation (Contract No. 102340406022150260476040).

*E-mail address: zhaojj@dlut.edu.cn

[1] C. T. Foxon and B. A. Joyee, Surf. Sci. **50**, 434 (1975); **64**, 293 (1975).
[2] C. Gaicia, C. Neri, and J. Massies, J. Cryst. Growth **98**, 511 (1989).
[3] Y. Fukunishi and H. Nakatsuji, Surf. Sci. **291**, 271 (1993); **291**, 271 (1993); **316**, 168 (1994).
[4] K. Shiraishi and T. Ito, Surf. Sci. **357**, 451 (1996).
[5] *Clusters of Atoms and Molecules I*, edited by H. Haberland (Springer-Verlag, Berlin, 1995).
[6] R. L. Johnston, *Atomic and Molecular Clusters* (Tylor & Francis, London, 2002).
[7] *Molecular Clusters of the Main Group Elements*, edited by M. Driess and H. Nöth (Wiley-VCH, Weinheim, 2004).
[8] J. Donohue, *The Structures of the Elements* (Wiley, New York, 1974).
[9] S. L. Bennett, J. L. Margrave, J. L. Franklin, and J. E. Hunson, J. Chem. Phys. **59**, 5814 (1973).
[10] Y. Morino, T. Ukaji, and T. Ito, Bull. Chem. Soc. Jpn. **39**, 64 (1966).
[11] S. B. Brumbach and G. M. Rosenblatt, J. Chem. Phys. **56**, 3110 (1972).
[12] Y. M. Bosworth, R. J. H. Clark, and D. M. Rippon, J. Mol. Spectrosc. **46**, 20 (1973).
[13] L. S. Wang, Y. T. Lee, D. A. Shirley, K. Balasubramanian, and P. Feng, J. Chem. Phys. **93**, 6310 (1990).
[14] L. S. Wang, B. Liu, Y. T. Lee, D. A. Shirley, E. Ghelichkhani, and E. R. Grant, J. Chem. Phys. **93**, 6318 (1990).
[15] L. S. Wang, B. Liu, Y. T. Lee, D. A. Shirley, E. Ghelichkhani, and E. R. Grant, J. Chem. Phys. **93**, 6327 (1990).
[16] H. J. Zhai, L. S. Wang, A. E. Kuznetsov, and A. I. Boldyrev, J. Phys. Chem. A **106**, 5600 (2002).
[17] T. P. Lippa, S. J. Xu, S. A. Lyapustina, J. M. Nilles, and K. H. Bowen, J. Chem. Phys. **109**, 10727 (1998).
[18] R. K. Yoo, B. Ruscic, and J. Berkowitz, J. Chem. Phys. **96**, 6696 (1992).
[19] J. A. Zimmerman, S. B. H. Bach, C. H. Watson, and J. R. Eyler, J. Phys. Chem. **95**, 98 (1991).
[20] K. Balasubramanian, K. Sumathi, and D. Dai, J. Chem. Phys. **95**, 3494 (1991).
[21] U. Meier, S. D. Peyerimhoff, and F. Grein, Chem. Phys. **150**, 331 (1991).
[22] J. J. BelBruno, Heteroat. Chem. **14**, 189 (2003).
[23] Y. Zhao, W. Xu, Q. Li, Y. Xie, and H. F. Schaefer III, J. Comput. Chem. **25**, 907 (2004).
[24] G. Igel-Mann, H. Stoll, and H. Preuss, Mol. Phys. **80**, 325 (1993).
[25] D. S. Warren, B. M. Gimarc, and M. Zhao, Inorg. Chem. **33**, 710 (1994).
[26] P. Ballone and R. O. Jones, J. Chem. Phys. **100**, 4941 (1994).
[27] M. Shen and H. F. Schaefer III, J. Chem. Phys. **101**, 2261 (1994).
[28] T. Baruah, M. R. Pederson, R. R. Zope, and M. R. Beltran, Chem. Phys. Lett. **387**, 476 (2004).
[29] M. J. Moses, J. C. Fettinger, and B. W. Eichhorn, Science **300**, 778 (2003).
[30] T. Baruah, R. R. Zope, S. L. Richardson, and M. R. Pederson, Phys. Rev. B **68**, 241404(R) (2003).
[31] J. J. Zhao and R. H. Xie, Chem. Phys. Lett. **396**, 161 (2004).
[32] M. Haser, U. Schneider, and R. Ahlrichs, J. Am. Chem. Soc. **114**, 9551 (1992).
[33] M. Haser and O. Treutler, J. Chem. Phys. **102**, 3703 (1995).
[34] J. P. Perdew, K. Burke, and M. Ernzerhof, Phys. Rev. Lett. **77**, 3865 (1996).
[35] DMOL is a density functional theory (DFT) package based atomic basis distributed by Accelrys. B. Delley, J. Chem. Phys. **92**, 508 (1990).
[36] F. H. Stillinger and T. A. Weber, Phys. Rev. B **31**, 5262 (1985).
[37] D. M. Deaven and K. M. Ho, Phys. Rev. Lett. **75**, 288 (1995).
[38] J. J. Zhao and R. H. Xie, J. Comput. Theor. Nanosci. **1**, 117 (2004).
[39] Y. H. Luo, J. J. Zhao, S. T. Qiu, and G. H. Wang, Phys. Rev. B **59**, 14903 (1999); J. J. Zhao, Y. H. Luo, and G. H. Wang, Eur. Phys. J. D **14**, 309 (2001).
[40] J. J. Zhao, Phys. Rev. A **64**, 043204 (2001); J. L. Wang, G. H.

Wang, and J. J. Zhao, Phys. Rev. B **64**, 205411 (2001); J. L. Wang, G. H. Wang, and J. J. Zhao, J. Phys.: Condens. Matter **13**, L753 (2001); J. L. Wang, G. H. Wang, and J. J. Zhao, Phys. Rev. B **66**, 035418 (2002); J. L. Wang, G. H. Wang, and J. J. Zhao, Phys. Rev. A **68**, 013201 (2003); B. L. Wang, X. S. Chen, G. B. Chen, G. H. Wang, and J. J. Zhao, Surf. Rev. Lett. **11**, 15 (2004); S. Yoo, J. J. Zhao, J. L. Wang, and X. C. Zeng, J. Am. Chem. Soc. **126**, 13845 (2004); B. L. Wang, J. J. Zhao, X. S. Chen, D. N. Shi, and G. H. Wang, Phys. Rev. A **71**, 033201 (2005); X. L. Zhou, J. J. Zhao, X. S. Chen, and W. Lu, *ibid.* **72**, 053203 (2005).

[41] R. O. Jones and D. Hohl, J. Chem. Phys. **92**, 6710 (1990); R. O. Jones and G. Seifert, *ibid.* **92**, 7564 (1992).

[42] K. P. Huber and G. Herzberg, *Molecular Spectra and Molecular Structure: Vol. IV; Constants of Diatomic Molecules* (Van Nostrand Reinhold, New York, 1979).

[43] T. K. Ha, O. Suleimenov, and M. T. Nguyen, Chem. Phys. Lett. **315**, 327 (1999); F. J. Owens, J. Mol. Struct.: THEOCHEM **623**, 197 (2003).

[44] G. Seifert, T. Heine, and P. W. Fowler, Eur. Phys. J. D **16**, 341 (2001).

[45] J. G. Han and J. A. Morales, Chem. Phys. Lett. **396**, 27 (2004).

[46] L. Apker, E. Taft, and J. Dickey, Phys. Rev. **76**, 270 (1949).

[47] Z. Q. Wang and D. Stroud, Phys. Rev. B **42**, 5353 (1990).